Journal of Power Sources 256 (2014) 383–393

Contents lists available at ScienceDirect

Journal of Power Sources

journal homepage: www.elsevier.com/locate/jpowsour

Insight into the structural construction of a perfluorosulfonic acid membrane derived from a polymeric dispersion

Zhao Wang, Haolin Tang*, Junrui Li, Yan Zeng, Lutang Chen, Mu Pan

State Key Laboratory of Advanced Technology for Materials Synthesis and Processing, Wuhan University of Technology, Wuhan 430070, PR China

HIGHLIGHTS

- Performance and microstructure of perfluorosulfonic membrane is depended on the solvents.
- Nafion aggregation decrease with the increase of the dielectric constant.
- Nafion aggregation decrease with the decrease of solubility parameters gap.

GRAPHICAL ABSTRACT

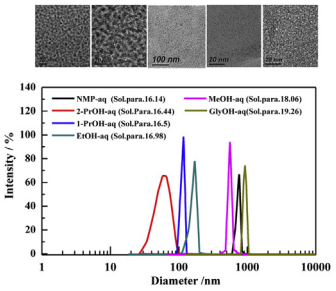

ARTICLE INFO

Article history:
Received 1 November 2013
Received in revised form
17 January 2014
Accepted 21 January 2014
Available online 29 January 2014

Keywords:
Proton exchange membrane
Structural construction
Polymeric dispersion
Dielectric constant
Solubility parameter

ABSTRACT

The effects of the nature of the solvent on the morphology of perfluorosulfonate ionomers in dispersions and the microstructures of the corresponding formed membranes are investigated. The subsequent electrochemical performances of the formed proton exchange membranes are also studied in detail. It is found that the diameters of the Nafion molecular aggregates in variable solutions decrease with an increase in the solvent dielectric constant (ε) and a decrease in the gap of the solubility parameters (δ) between the resin and the solvent. The micromorphology of Nafion is further examined by means of transmission electron microscopy, small-angle X-ray scattering, and X-ray diffraction. It is found that the membrane cast from a Nafion-2-propanol/water dispersion with ε value of 42.38 and a δ gap of 0.01 (cal cm^{-3})$^{1/2}$ has a better ion cluster arrangement, smaller ion cluster size (approximately 13 Å), and higher crystallinity (16.7%) than the other samples. The electrochemical properties of the formed membranes are further investigated as a function of temperature, relative humidity, and the solubility parameter of the applied solvents. The results demonstrate that the electrochemical performance is strongly influenced by the solvent-induced microstructure of the backbone and the ionic clusters in the perfluorosulfonic acid membrane.

© 2014 Elsevier B.V. All rights reserved.

1. Introduction

Perfluorosulfonic acid (PFSA) ionomers such as Nafion have been extensively used in proton exchange membrane fuel cells as a polymer electrolyte and separator between the cathode and the anode because of their high structural stability and superior electrochemical properties in the hydrated state [1,2]. Generally, the technique for preparing a Nafion membrane is the solution-cast method, with which Nafion solutions are added to a desired container and then the solvent is allowed to evaporate to form the membrane through a particular thermal process [3]. Therefore, detailed information about the Nafion ionomer dispersion is crucial and helpful for achieving a better understanding of the nature and microstructure of the membrane that forms [4,5].

Nafion is a copolymer with comb-like structure that contains a hydrophobic poly(tetrafluoroethylene) (PTFE) backbone and

* Corresponding author. Tel.: +86 27 8788 4448; fax: +86 27 8787 9468.
E-mail addresses: thln@whut.edu.cn, haolin.tang@yahoo.com (H. Tang).

0378-7753/$ – see front matter © 2014 Elsevier B.V. All rights reserved.
http://dx.doi.org/10.1016/j.jpowsour.2014.01.096

perfluorovinyl ether side chains terminated with hydrophilic sulfonate groups. It is, therefore, not surprising that a degree of phase separation occurs in the hydrated Nafion membrane, which leads to the formation of interconnected, hydrated ionic clusters inside the membrane that determine the electrochemical properties of the membrane. The mechanical strength of the Nafion membranes is also improved through the crosslinking of the perfluorinated backbones induced by thermal treatment during the membrane formation process [6]. In the 1970s, the cohesive energy density of Nafion was determined experimentally from swelling measurements using the method developed by Britow and Watson [7]. The results showed that there are two distinct swelling envelopes corresponding to dual cohesive energy densities: one is ascribed to the organic part of the membrane, whereas the other is tentatively attributed to the ion clusters within the material. It was reported that the conformation of the Nafion molecules in solution depends strongly on the dielectric constant and the solubility parameter of the solvent that was used [8]. Ubbelohde viscosity measurements showed that dilute solutions of the perfluorosulfonated ionomer in various solvents exhibited quite different dielectric constants. For alcoholic and aqueous solutions of Nafion, an enhanced "polyelectrolyte effect" was observed with an increase in the dielectric constant of the solvent; however, this polyelectrolyte effect was not significant for other highly polar solvents [9]. It was also observed that the zeta potential of the Nafion dispersion, which reflects the aggregation status of the ionomer molecules, strongly depends on the concentration of the molecules. When the concentration of Nafion was varied from 0.5 to 1 wt%, the zeta potential increased significantly from approximately 0–12 mV, which corresponds to a change in the structure of the Nafion molecules from a true solution to a dispersion [10]. In addition, the conformation and the structure of the perfluorosulfonated ionomer in polar solvents such as alcohols, amides, and water have also been investigated using small-angle neutron scattering (SANS) and small-angle X-ray scattering (SAXS) [11–16]. In general, two Nafion molecular aggregation processes in alcoholic or aqueous solutions have been proposed based on the scattering data [17]. The primary aggregation induced by the hydrophobic interaction of the perfluorocarbon backbone can lead to the formation of rod-like aggregated particles with sizes of several hundred nanometers. It is worth noting that the primary aggregated particles can be dissociated into single molecular chains by further diluting the dispersion. The secondary aggregation process is attributed to the ionic aggregation of primary aggregated particles induced by the electrostatic attraction of the Nafion side chain $-SO_3^-$ ion pairs, which leads to the formation of large aggregated particles with sizes of approximately 10^4 nm. Thus, a cylinder-like conformation of Nafion is expected in solution, where the aggregated perfluorocarbon backbones form the compact cylinders and the sulfonated vinylether side chains are located at the polymer/solvent interface. Moreover, the dispersion properties could affect the microstructure of the membrane that forms. Accordingly, the conductivities and transport selectivities of the membranes that form, which are related to the membrane electrode assembly performance, are also dependent on the dispersion properties of Nafion. Therefore, it is of great importance to understand the dispersion properties of the Nafion ionomer used in PEMs.

The unique construction and properties of Nafion membranes are believed to be closely related to the microscopic phase separation of the ionic parts ($-SO_3H$ groups) from the fluorocarbon matrix. Although the conformation of Nafion has been well studied with respect to its cation form, equivalent weight, and water content [18–24], the effect of the applied solvent on the conformation of the Nafion molecules and the microstructure of the subsequently formed membrane have not been reported. In this paper, we evaluated the structures of the perfluorosulfonic acid membranes formed by casting Nafion resin from different solvents, including methanol, ethanol, 2-propanol, 1-propanol, glycerol, and *N*-Methyl pyrrolidone. The influence of the solvent's properties, e.g., the polarity and the solubility parameter, on the dispersive behavior of the perfluorosulfonate ionomers, the ionic aggregate size, and the crystallinity is the main focus of this work. In addition, the relationship between the dispersive behavior of the Nafion sol and the proton conductivity of the membrane formed under various conditions, the activation energy of the proton transportation, and the stability of the physical structure of the formed membranes are also discussed in this study.

2. Experimental section

2.1. Preparation and characterization of the Nafion solutions

Nafion dispersion (EW1000), which contains 5 wt% of perfluorosulfonate resin (H^+ form) and 95 wt% of an isopropanol/water mixture (10:9 weight ratio), was purchased from DuPont Ind. Co. The Nafion solutions used in this study were prepared by the following procedure. To 500 mL of the commercial Nafion dispersion, 500 mL of deionized water was added. The mixture was concentrated to approximately 250 mL by evaporation of the solvent at 60 °C using a hot plate. To the resulting solution, 500 mL of deionized water was added, and solvent evaporation was carried out again. This process was repeated 3 more times to make sure that the isopropanol was removed from the Nafion solution. The final Nafion concentration in the aqueous solution was 10.63 wt%, which was checked by casting 100 mL of the Nafion aqueous solution to form a membrane and then titrating the EW value. The resultant Nafion aqueous solution was then diluted with the desired solvent, and that solution was then used for the preparation of the membranes. Six prepared Nafion solutions with different mixtures of solvents and the properties of those applied solvents, including the solubility parameters (δ) and dielectric constants (ε), are shown in Table 1. For comparison, the δ and ε of the single solvents and the Nafion resin are presented in Table 2. The final prepared solutions, which contained new solvents for the preparation of the membranes, had a Nafion concentration of 3 wt%.

Samples for transmission electron microscopy (TEM) were prepared according to the following method: to make a relatively thin film for TEM examination, carbon-coated grids were soaked in 1 wt% Nafion solutions, and the liquid was removed after 30 s using filter paper. A thin layer remained, which was then quickly dried to form a Nafion film with an estimated thickness of 30–50 nm. After that, the carbon-coated grids with thin Nafion membranes on the surface were stained by soaking them in 0.1 mol L^{-1} mercury nitrate solutions for 15 min and then washing them with deionized water. The images were obtained using a Hitachi H7600 microscope with an acceleration voltage of 80 kV. Image J software was used for the analysis of the obtained micrographs.

Dynamic light scattering (DSL) measurements were carried out with a Malvern HPPS Laser Particle Size Analyzer (Malvern, UK)

Table 1
Mixed solvents used for preparation of Nafion solutions in this study and their solubility parameters and dielectric constants.

Mixed solvent (6/4, v/v)	Abbreviation	δ/(cal $cm^{-3})^{1/2}$	ε
N-Methyl-2-pyrrolidone/water	NMP-aq	16.14	50.6
2-Propanol/water	2-PrOH-aq	16.44	42.38
1-Propanol/water	1-PrOH-aq	16.5	44.72
Ethanol/water	EtOH-aq	16.98	46.82
Methanol/water	MeOH-aq	18.06	50
Glycerol/water	GlyOH-aq	19.26	65

Table 2
Samples of Nafion solutions used herein and solubility parameters and dielectric constants of applied solvents.

Solvent	δ/(cal cm^{-3})$^{1/2}$	ε
NMP	11.3	32
2-Propanol	11.8 [15]	19.9
N-Propanol	11.9	22.2
Ethanol	12.7 [15]	24.5
Methanol	14.5 [15]	32.7
Glycerol	16.5	56
Water	23.4	78.5
Nafion backbone [7]	9.7	2.1
Nafion side chain [7]	16.45	15

with a scattering angle of 90° at 25 °C using a He–Ne laser (633 nm). To observe the particle sizes of the Nafion in different solvents clearly and accurately, the solutions prepared as described above that had 3 wt% of Nafion were diluted to 1 mg mL^{-1}. The diluted Nafion solutions were then filtered through a Millipore HWAP filter to remove dust and were left standing for 3 h before the DSL testing. These diluted solutions were also tested by small-angle X-ray scattering (SAXS).

2.2. Preparation and characterization of the Nafion membranes

Nafion membranes with a thickness of approximately 25 ± 1 μm were prepared using a recasting process. The pH of the Nafion solutions (3 wt% of resin) in different solvents, prepared as described in Experimental section 2.1, was adjusted to 7.0 using a 0.1 M NaOH aqueous solution, and the solution was recast using a Petri dish, followed by heat-treatment at 130 °C for 5 h and then at 200 °C for 3 h. The as-prepared membranes were then treated, using a standard procedure, for 30 min in a 5 wt% H_2O_2 solution at 80 °C, for 30 min in distilled water at 80 °C, for 30 min in a 0.5 mL L^{-1} H_2SO_4 solution at 80 °C, and finally for 30 min in distilled water at 80 °C again.

The tensile strength tests were performed on an electronic universal testing machine (WDW-0.5 type, Shanghai Hualong) at room temperature under 25% RH. The membranes were cut into rectangular samples with the dimensions of 60 mm × 5 mm. The samples were pulled by the machine along their longitudinal direction. The gauge length and tensile rate were 40 mm and 50 mm min^{-1}, respectively. The shrinkage stress generated by dehydrating the membrane from a saturated condition to 25% RH at 25 °C was also determined using samples of the same size.

X-ray diffraction (XRD) experiments were performed on a D/MAX-RB type diffractometer using a Cu Kα source at 40 mA and 40 kV. The scan range was 10–70°, and the scan rate was 4° min^{-1}. The amorphous peak was resolved into a crystalline peak and an amorphous peak using the Gaussian equation [25,26] after background correction. The crystallinity of the membrane was then calculated using the following equation:

$$X_c = \frac{\int_0^\infty I_c(q)q^2 \mathrm{d}q}{\int_0^\infty \left[I_c(q)q^2 + I_a(q)q^2\right]\mathrm{d}q} \quad (1)$$

$$q = \frac{4\pi}{\lambda \sin(\theta/2)} \quad (2)$$

where X_c is the crystallinity of membrane, q is the diffraction vector, λ is the wavelength of the Cu Kα radiation, θ is the diffraction angle, $I_c(q)$ is the sum of the intensities of the fitted crystalline peak, and $I_a(q)$ is the sum of the intensities of the fitted amorphous peak.

The in-plane proton conductivity of the prepared membranes was measured using an impedance analyzer (Autolab PG30/FRA, Eco Chemie, Netherlands) under various temperatures and RHs. Humidity was maintained by controlling the temperature of humidified gas before the gas was allowed to pass through the sample chamber. The membrane samples were equilibrated for 4 h at constant temperature and humidity. The membrane (6 cm × 1 cm) was sandwiched between two Pt sheets and the conductivity measurements were carried out with the electric field parallel to the membrane surface. One Pt sheet was used as the working electrode and the other as the reference and counter electrodes. The EIS was measured over the frequency range of 10 Hz–100 kHz with signal amplitude of 10 mV. The proton conduction was recorded after stabilizing the membranes under the test conditions for at least 30 min.

The single cell performances of the proton exchange membranes made from different solvents were tested on a G50 Fuel Cell Test Station (GreenLight) at 65 °C, without back pressure, using H_2 as the fuel and air as the oxidant. The Nafion 211 membrane (Du Pont Dispersion-Cast membrane, ~25 μm) was also tested as a reference. The fuel cell was assembled as follows. First, a catalyst layer consisting of Pt/C (60 wt% Pt/C, Johnson Matthey) and the Nafion ionomer was transferred to the membrane surface to obtain a catalyst coated membrane (CCM) [27]. The Pt loadings for the anode and the cathode were 0.15 mg cm^{-2} and 0.25 mg cm^{-2}, respectively. A gas diffusion layer (GDL) was placed on both sides of the CCM to form a membrane-electrode assembly (MEA). The MEA was mounted in a single cell test fixture with a serpentine flow field and a fuel cell clamp (with an active area of 25 cm^2). The stoichiometries for the anode (H_2) and cathode (air) were set as 1.5 and 2.5, respectively. Prior to measurement, the cells were activated by increasing the current density at the rate of 25 mA cm^{-2} per 2 min until the polarization curve is decreased to 0.2 V. After stabilizing under the corresponding current density for 30 min, the current density decreased to 0 mA cm^{-2} at the rate of 25 mA cm^{-2} per 2 min, keeping this circulation until stable performance was reached. The polarization curve was recorded until the performance reached a stable state at each testing point.

The gas permeability or crossover through the Nafion membranes of the single cell was tested in situ using an Agilent chromatograph, GC 6890. The chromatography system was equipped with a Mass Selective Detector 5975 and used high purity argon (99.999%) as the carrier gas.

3. Results and discussion

3.1. Micro-morphology of Nafion in dilute solutions

Fig. 1a–m displays high-resolution TEM images of the backbone aggregation and the ion cluster morphology of 1 wt% Nafion in different solvents. According to the TEM images in Fig. 1, three phases existed in the Nafion membrane: the ionic cluster phase (black points), the organic matrix phase (white areas), and the interfacial phase (gray areas), and this finding is consistent with the literature [28–32]. Each phase, which can be distinguished by its brightness in the TEM images, was homogeneously dispersed throughout the membrane. However, the size of the ionic domains and the morphology of the proton transport channels in the perfluorosulfonic acid membrane varied as the solvent was changed. Because the only variable was the applied solvent and all of the other factors were the same during the preparation processes of the samples, the differences in the morphologies of the Nafion molecules in the solutions were attributed to the different solvents that

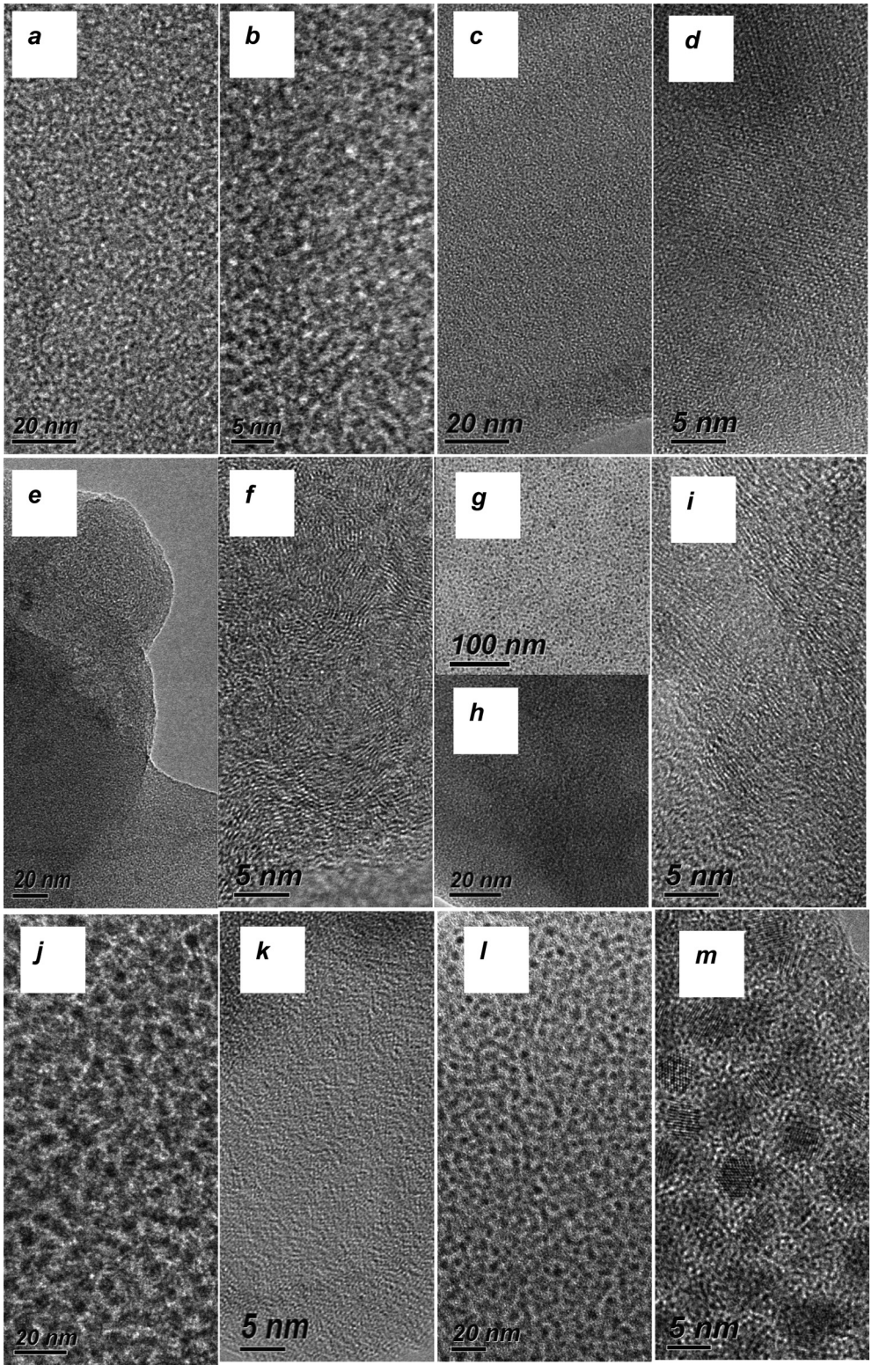

Fig. 1. High resolution TEM images of the Nafion in different solvents: MeOH-aq (a, b), 2-PrOH-aq (c, d), 1-PrOH-aq (e, f), EtOH-aq (g, h,i), NMP-aq (j, k), GlyOH-aq (l, m).

were applied. The dielectric constant and Hansen solubility parameters (HSP) [33] are important properties of various substances and are useful tools for the selection of their solvents or in the prediction of their behavior in numerous applications. The design and evaluation of these parameters relies on the basic rule of "similarity matching" for solubility [34]. As a result, the sizes of the ionic domains and the morphologies of proton transport channels in the perfluorosulfonic acid membranes are closely related with the solubility parameters (δ) and dielectric constants (ε) of the solvents. As can be seen from Table 2, the solubility parameters of the backbone and side chain are 9.7 (cal $cm^{-3})^{1/2}$ and 16.45 (cal $cm^{-3})^{1/2}$, and the dielectric constants (ε) are 2.1 and 15,

respectively. Fig. 1c, d presents the micro-morphology of the Nafion in the 2-propanol/water. It can be seen from Fig. 1c, d that the ionic clusters (black points) were distributed uniformly and orderly throughout the membrane. Because the solubility parameter gap between 2-PrOH-aq and Nafion is only 0.01 (cal cm^{-3})$^{1/2}$ and because the dielectric constant of 2-PrOH-aq (42.38) is high enough, the molecular chains of Nafion can be dispersed well in this mixed solvent. With an increase in the solubility parameter gap between the solvent and Nafion, i.e., 0.05, 0.53, 0.31, 1.61 and 2.81 for 1-PrOH-aq, EtOH-aq, NMP-aq, MeOH-aq, and GlyOH-aq, respectively, the ionic cluster and the structure of its construction varied from a regular distribution and linear arrangement (Fig. 1f, i) to a random dispersion (Fig. 1k), and the size of ionic cluster also increased (Fig. 1b, m). In addition, when the comparison between Fig. 1a, j, l and Fig. 1c, g, e is made, combined with the ε values in Table 1, it can be seen that the solvent with a higher ε can contribute to the formation of PFSA ionic aggregation much more than those solvents with lower ε values. This phenomenon also agrees with the concept that "polar molecules are soluble in polar solvents" in the "similarity matching" theory [18,34].

To further determine the conformation of Nafion in different solvents, dynamic light scattering (DSL) measurements were performed for samples containing 1 wt% of Nafion. The relationship between the hydrodynamic diameter of Nafion and the nature of the solvents is presented in Fig. 2. It can be clearly seen that the hydrodynamic diameter of Nafion in the 2-PrOH-aq solution is approximately 57 nm, which corresponds to single molecules [35]. The hydrodynamic diameters of Nafion in MeOH-aq, EtOH-aq, 1-PrOH-aq, NMP-aq, and GlyOH-aq are 880 nm, 287 nm, 133 nm, 442 nm, 927 nm, respectively. The sizes of the aggregated Nafion particles in solvents decrease sequentially in the following order: GlyOH-aq > MeOH-aq > NMP-aq > EtOH-aq > 1-PrOH-aq > 2-PrOH-aq. This behavior has also been investigated in a very similar system using dynamic light scattering measurements by Ma et al. [18], who proposed that the perfluorocarbon backbones of the Nafion aggregate and form a mixture of rectangle-like and cube-like structures in MeOH-aq, EtOH-aq, and 2-PrOH-aq with the sulfonate groups on the side chains located at the polymer/solvent interface. These results demonstrated that the aggregation of Nafion in solution is strongly affected by the nature of the applied solvent. The Nafion aggregate size in the solution decreases if the ε of the solvent is higher than that of Nafion and if the δ of the solvent is close to that of Nafion. Moreover, the δ of the solvent plays a dominating role in determining the size of the Nafion molecules if the ε of the solvent is higher than that of the side chains of Nafion.

It is well-known that water-coordinated proton transport through the membrane is affected by the volume of water around the sulfonate groups in the membrane [37]. To understand whether the membrane morphology has any significant effect on its electrochemical performance [38], the ionic cluster structures of Nafion in various solvents were investigated using the SAXS technique. The results are presented in Fig. 3a. The average ion cluster dimension in the membrane was calculated from the following equation [39]:

$$d = \frac{2\pi}{q} \tag{3}$$

where d is the average ion cluster dimension in the membrane (angstroms) and q is the scattering vector (angstroms), respectively.

Fig. 3a shows the scattering data of Nafion molecules in different solvents. The cluster size of Nafion in each solvent was calculated using equation (3), and the effect of the solubility parameters on the ion cluster size is presented in Fig. 3b. The cluster sizes of the Nafion molecules in 2-PrOH-aq, 1-PrOH-aq, EtOH-aq, MeOH-aq, NMP-aq, GlyOH-aq were 13.08, 13.65, 15.7, 20.26, 17.94 and 24.15 Å, respectively. According to Fig. 3b, it can be concluded that the wider the solubility parameter gap between the solvent and Nafion if the ε of the solvent is higher than that of the side chains of Nafion, the bigger the cluster particles are formed [39,40], which is consistent with previous TEM observations.

The relationship between the nature of solvent and the hydrodynamic diameters/cluster size are showed in Fig. 3b–e. As it can been seen from Fig. 3b, c, the hydrodynamic diameter and cluster size of Nafion increased with the increased gap between the solubility parameter of solvent and the solubility parameter of Nafion (16.45 (cal cm^3)$^{-1/2}$). As a result, the hydrodynamic diameter/cluster size of Nafion in the solvent of 2-PrOH is the smallest (57 nm/13.08 A) in these samples, and the largest size (927 nm/24.15 A) belongs to the GlyOH-aq which has the gap of solubility parameter of 2.81 (cal cm^3)$^{-1/2}$. These results indicate that the solubility parameter of solvent is one of the most important factors for the size of Nafion. Considering the dielectric constant of solvents (Fig. 3d, e), both the size of ion cluster and the hydrodynamic diameter of Nafion exhibit ascending trends with the increase in dielectric constant. This result is attributed to the polarity of the applied solvents. Their dielectric constants (42.38, 44.72, 46.82, 50, 50.6 and 65 for 2-PrOH-aq, 1-PrOH-aq, EtOH-aq, MeOH-aq, NMP-aq and GlyOH-aq, respectively) are much bigger than that of Nafion (2.1 for backbone and 15 for side chain). Thus, the dielectric constants become an insignificant factor for the hydrodynamic diameter and clusters size. Since the gap of solubility parameter between NMP-aq and Nafion is 0.31 (cal cm^3)$^{-1/2}$, which is less than one fifth of the gap of solubility parameter between MeOH-aq and Nafion (1.61 (cal cm^3)$^{-1/2}$), the hydrodynamic diameter and the clusters size of Nafion in NMP-aq (442 nm/17.94 A) are much smaller than that of in MeOH-aq (880 nm/20.26 A). These results also agree with that the δ of the solvent plays a dominating role in determining the size of the Nafion molecules if the δ of the solvent is higher than that of the side chains of Nafion.

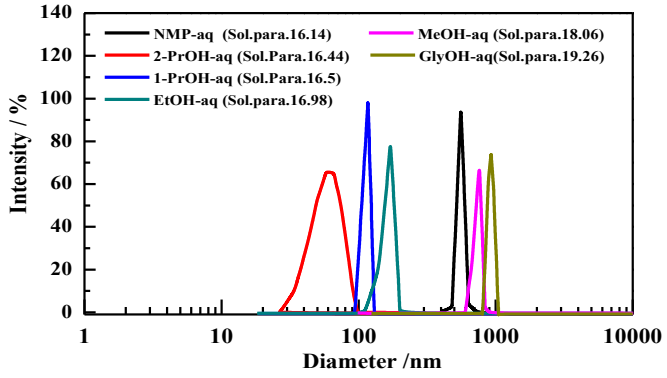

Fig. 2. Particles size of Nafion in solvents with different solubility parameter and dielectric constants.

3.2. Effect of the solvent on the electrochemical performance of the Nafion membranes

Fig. 4a–c reveals the proton transport mechanism under different relative humidities (including 100%, 50%, and 30%) by displaying the connection among the proton conductivity, the nature of the solution, and the temperatures. Currently, there are two main proton transport mechanisms [41,42]. The Grotthuss mechanism suggests that a proton diffuses through the hydrogen bonded network of water molecules via the formation or cleavage of covalent bonds [42]. The vehicle mechanism holds the point of view that proton movement takes place with the aid of a moving "vehicle", e.g., H_2O as the complex ion H_3O^+ [24]. It can be

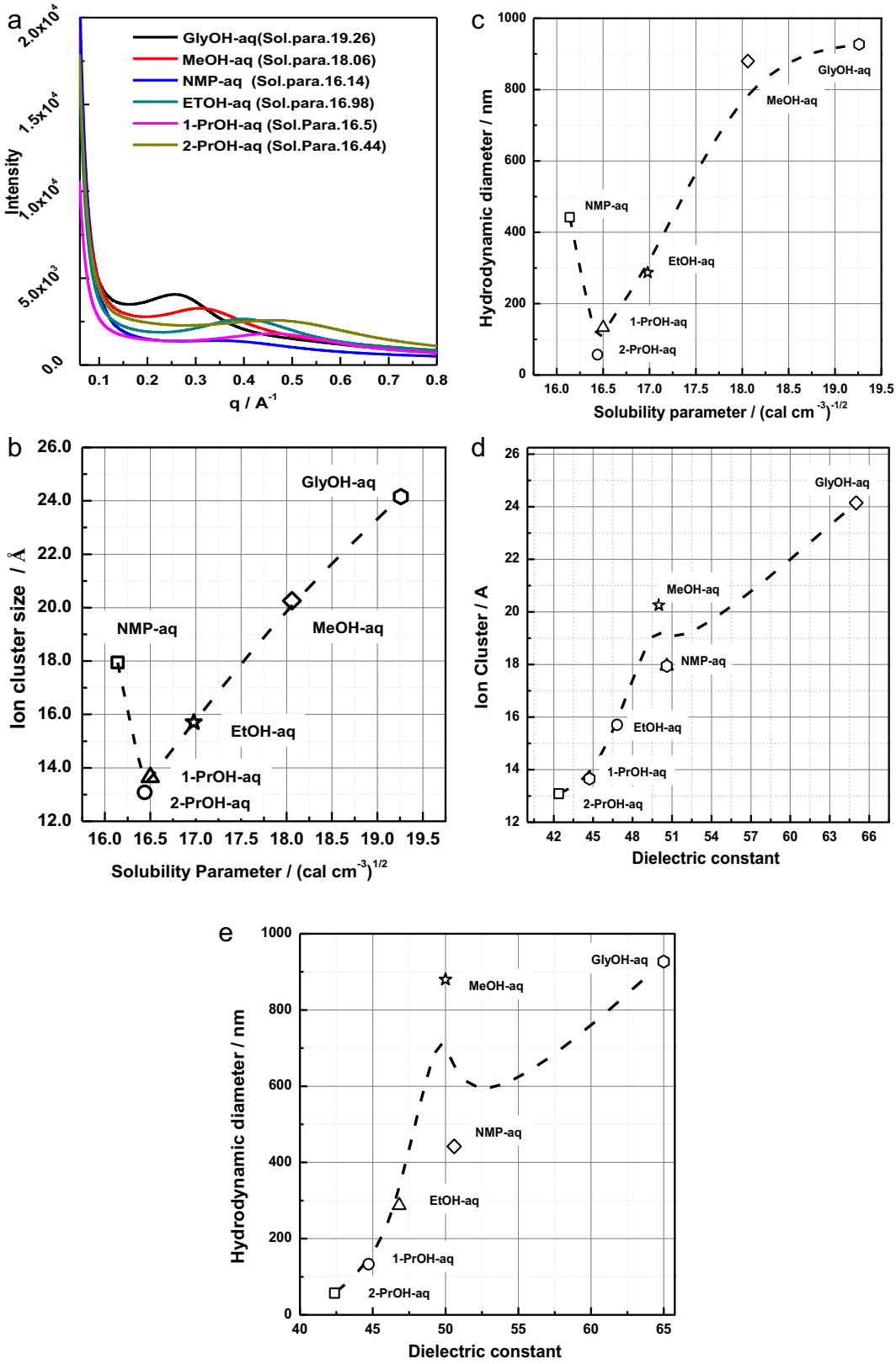

Fig. 3. SAXS of the Nafion microstructure (a), the cluster size of Nafion vs the solubility parameter (b), the hydrodynamic diameter of Nafion vs the solubility parameter (c), the cluster size of Nafion vs the dielectric constant (d), the hydrodynamic diameter of Nafion vs the dielectric constant (e).

concluded from these two main mechanisms that the water content in a proton exchange membrane has a great effect on its electrochemical performance, as shown in Fig. 4a–c and confirmed by other scientists [34,36]. Moreover, two main types of water exist in the proton exchange membrane: absorbed water and free water [28,43,44].

Under 100% RH (Fig. 4a), the increase in the gas hydration tended to saturate the sulfonate groups, and thus, high conductivity

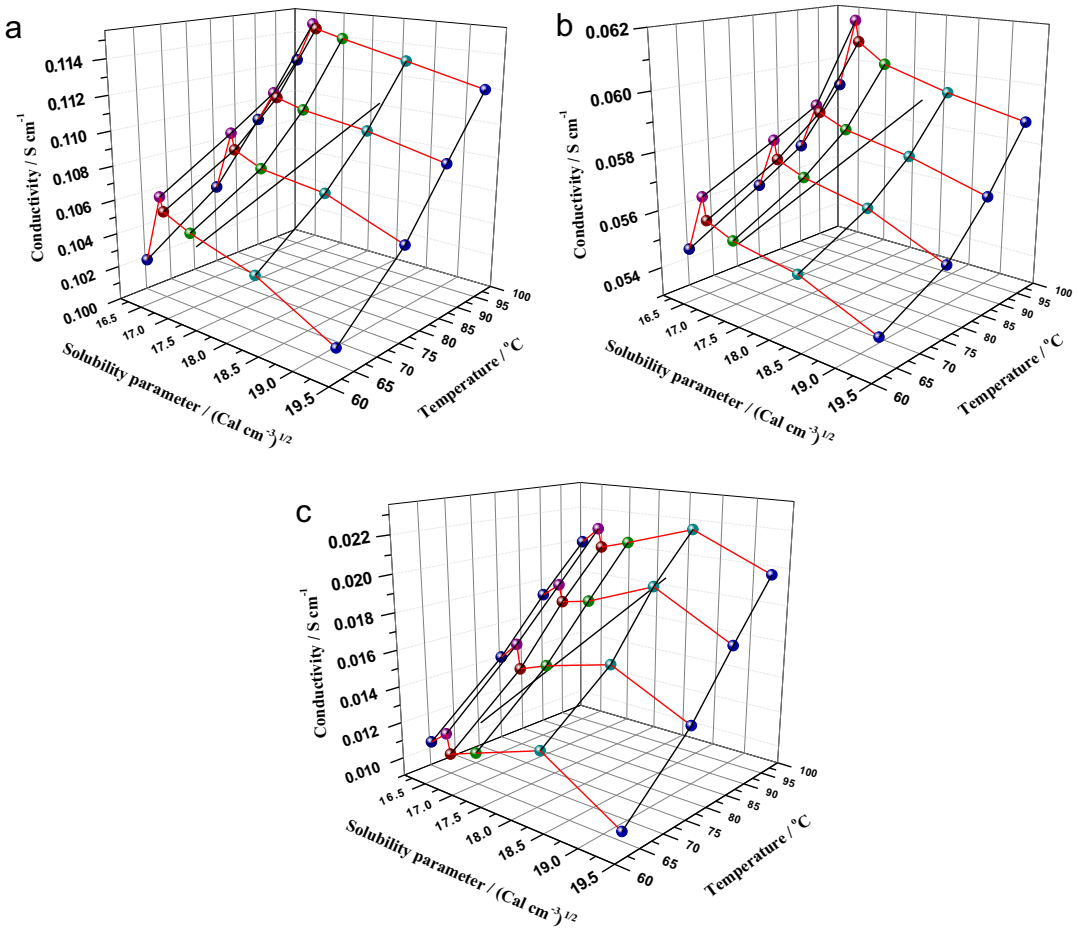

Fig. 4. Proton conductivities of the proton exchange membranes at varies temperatures and 100% RH (a), Proton conductivities of the proton exchange membranes at varies temperatures and 50% RH (b),Proton conductivities of the proton exchange membranes at varies temperatures and 30% RH (c).

values were achieved. The highest proton conductivity, which was 0.115 S cm^{-1} at 100 °C and 0.106 S cm^{-1} at 65 °C, was observed for the membrane made from the 2-propanol/water sol of Nafion. Although the differences in the proton conductivities of the membranes were generally small under high RHs, the effect of the solvent can be easily observed from Fig. 4a, and the proton conductivities decreased in the following order: 2-PrOH-aq > 1-PrOH-aq > EtOH-aq > NMP-aq > MeOH-aq > GlyOH-aq. K.D. Kreuer [45] made a comparison between the proton conductivity diffusion coefficient (D_σ) and the water diffusion coefficient (D_{H_2O}). It was found that the D_σ is higher than the D_{H_2O} when the RH is high enough, indicating that the proton was transferred by H_3O^+ (vehicle mechanism), and $-SO_3H$ (Grotthuss), simultaneously. However, under high RH working conditions, the amount of free water that existed in the Nafion membrane was much more than that of the absorbed water. In addition, the Grotthuss mechanism involves the cleavage and formation of hydrogen bonds [42], which leads to more energy consumption than the vehicle mechanism does. Thus, under conditions of high RH, the protons were probably transported through complex ions like H_3O^+, which are mobile as a whole [46]. With an increase in the water content inside the membrane, both the connectivity and the diameter of the proton conducting channels (ionic clusters) were enhanced [28]. Accordingly, the ionic conductivity increased with an increase in the water content inside the membrane. As shown in the TEM images, ionic clusters of Nafion in the 2-PrOH-aq solvent are well-dispersed, leading to an increased number of effective and low-sinuosity proton conducting channels. However, the ionic cluster distribution and the proton conducting channels in membranes made from 1-PrOH-aq, EtOH-aq, and NMP-aq are irregular, and slightly curved pathways for proton transport were formed. Accordingly, the proton conductivity values of those membranes were lower than that of the membrane made from 2-PrOH-aq. Moreover, due to the great solubility parameter gap between GlyOH-aq and Nafion, the proton conductivity of the membrane made from GlyOH-aq was the lowest among these six samples (0.111 S cm^{-1} at 100 °C and 0.100 S cm^{-1} at 65 °C).

G. Gebel [28] investigated the structural evolution of perfluorosulfonated ionomer membranes from dry materials to highly swollen membranes and solutions using the small-angle scattering technique. It was found that when the water content is close to 30 wt%, the cluster structure of Nafion consists of spherical ionic domains connected with cylinders of water dispersed in the polymer matrix. Thus, the less-connected spherical domains under RH below 30% results in the lower mobility of the side chain of Nafion and the fixed water molecules around SO_3^-, leading to decreased proton conductivity diffusion coefficient (D_σ) and the water diffusion coefficient (D_{H_2O}). Accordingly, the proton conductivity of Nafion decreased dramatically. Since and the D_σ is closed to D_{H_2O} at low RH [45], it can be concluded that the main way for proton transportation is governed by the Vehicular mechanism. The proton conductivity values of all six of these samples decreased

dramatically with a drop in the RH (Fig. 4b). The membrane made from the Nafion dispersion in 2-PrOH-aq exhibited a much higher conductivity than the other membranes because of its superior structure. Moreover, based on its large ionic clusters (Fig. 1i), the membrane cast from GlyOH-aq exhibited good performance in a low RH environment (Fig. 4c) (0.020 S cm^{-1} at 100 °C and 0.011 S cm^{-1} at 65 °C under 30% RH), which is close to the performance of the membrane cast from 2-PrOH-aq (from 0.021 S cm^{-1} at 100 °C and 0.012 S cm^{-1} at 65 °C under 30% RH).

Fig. 4b presents the proton conductivity values of the Nafion membranes at different temperatures under 50% RH. The conductivity of the membrane made from the Nafion dispersion in 2-PrOH-aq was 0.062 S cm^{-1} at 100 °C, which was higher than the values of the membranes made from Nafion dispersions in 1-PrOH-aq (0.061 S cm^{-1} at 100 °C), MeOH-aq (0.059 S cm^{-1} at 100 °C), NMP-aq (0.060 S cm^{-1} at 100 °C), and GlyOH-aq (0.059 S cm^{-1} at 100 °C). In addition, the conductivities of the membranes at other temperatures showed the same trend. Under intermediate RH conditions, the $-SO_3H$ in the membrane was surrounded by an abundance of absorbed water, and there was also a certain amount of free water molecules in the membrane that can act as a proton carrier, which indicates that the proton transport is governed by both "the Grotthuss mechanism" and "the vehicle mechanism" simultaneously.

The effect of the solubility parameter on cell performance was further investigated under different humidification levels. As shown in Fig. 5a, a single cell assembled with a membrane cast from 2-PrOH-aq showed a voltage of 0.608 V and at a current density of 1000 mA cm^{-2}, which was slightly higher than that of the cell assembled with a commercial Nafion 211 membrane (0.590 V). This superior performance should be partly ascribed to the membrane fabrication temperature of 200 °C. It has been reported that the annealing of the perfluorosulfonic acid electrolyte can change the electrolyte microstructure and increase the cell performance [47,48]. The influence of the casting solvents became obvious when comparing the four other samples. The cell voltages of cells assembled with membranes cast from EtOH-aq, NMP-aq, MeOH-aq and GlyOH-aq were 0.582 V, 0.561 V, 0.546 V and 0.528 V, respectively. In situ impedance suggested that the differences in the cell voltages of the single cells mainly resulted from the cell resistances. The cell resistances for the cells assembled with membranes cast from 2-PrOH-aq, 1-PrOH-aq, EtOH-aq, NMP-aq, MeOH-aq and GlyOH-aq were 1.289, 1.320, 1.340, 1.333, 1.360, 1.385 and 1.440 Ω, respectively, at a current density of 1000 mA cm^{-2}, and the order was consistent with that of the proton conductivities displayed in Fig. 4.

Differences in the performances of cells assembled from Nafion membranes cast from different solvents became significant when the humidity of the inlet gas was decreased. Fig. 5b shows the performances of single cells assembled with different types of Nafion membranes under inlet gas with 50% RH at 65 °C. According to Fig. 5b, the open circuit voltage (OCV) values are 0.982, 0.978, 0.974, 0.971, 0.967 and 0.962 V for single cells assembled with membranes cast from Nafion dispersions in 2-PrOH-aq, 1-PrOH-aq, EtOH-aq, NMP-aq, MeOH-aq and GlyOH-aq, respectively, compared to the Nafion 211 membrane, which had a value of 0.975 V. The voltage reduction rate in the ohmic polarization stage, which is represented by the current density between 600 and 1000 mA cm^{-2} in the Fig. 5b, decreased sequentially as follows for the membranes cast from GlyOH-aq > MeOH-aq > NMP-aq > EtOH-aq > 1-PrOH-aq > 2-PrOH-aq. The cell resistances for the cells assembled with membranes cast from 2-PrOH-aq, 1-PrOH-aq, EtOH-aq, NMP-aq, MeOH-aq and GlyOH-aq increased to 2.971, 3.136, 3.166, 3.326, and 3.446 Ω, respectively, at a current density of 1000 mA cm^{-2}. These results further demonstrate that the solvent

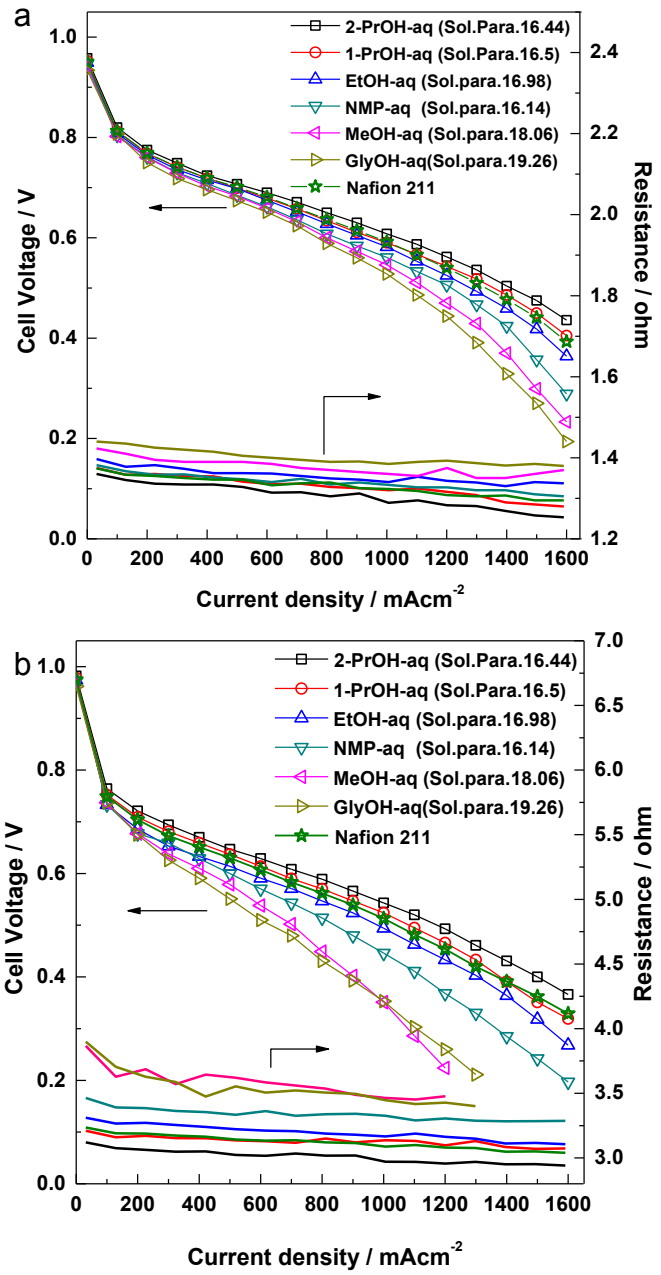

Fig. 5. Single cell performances of the proton exchange membranes at 65 °C and 100% RH (a), and 50% RH (b).

used for the formation of the membrane has a great effect on the structural density of the PFSA membrane, which was also observed by other researchers [49,50].

Moreover, the H_2 crossover of these single cells was also tested at 100% RH and 50% RH. It was observed that the H_2 crossover rate under high RH was much higher than that under low RH [51–53]. The crossover values of the Nafion 211 membrane at 100% RH and 50% RH were 3.174 and 2.543 mol cm^{-2} s^{-1}. This is also evidence that the OCV values of the membranes tested at 50% RH were higher than the values of those tested at 100% RH. The H_2 crossover values of membranes cast from various solvents are displayed in Fig. 6. It can be concluded that the H_2 crossover rate at 50% RH increased in the following order for membranes cast from 2-PrOH-aq (1.885 mol cm^{-2} s^{-1}), 1-PrOH-aq (2.072×10^{-9} mol cm^{-2} s^{-1}), EtOH-aq (2.499×10^{-9} mol cm^{-2} s^{-1}), NMP-aq (2.856 mol cm^{-2} s^{-1}),

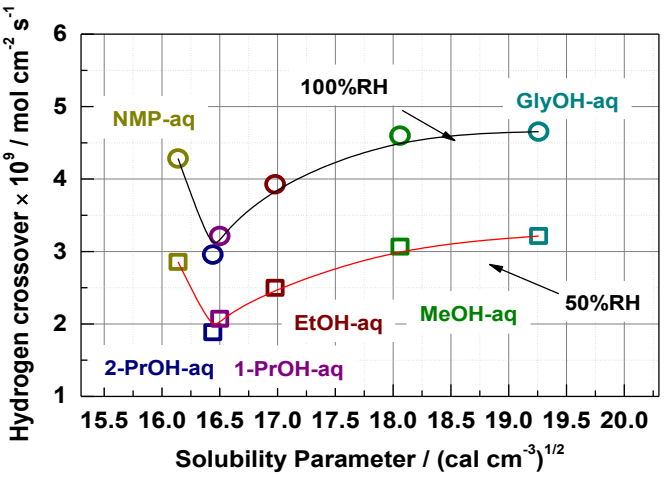

Fig. 6. The H_2 crossover performance of the proton exchange membranes casted from variable solvents, at 65 °C and 100% RH (□), and 50% RH (○).

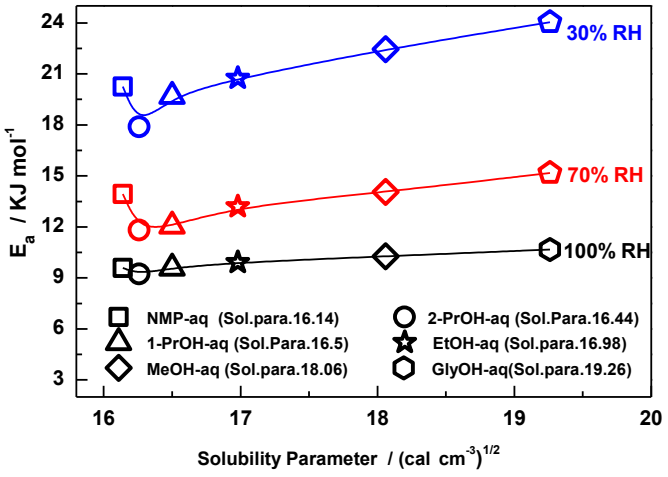

Fig. 7. The protonic conductivity activation energy of membranes in different RH.

MeOH-aq (3.067 mol cm^{-2} s^{-1}), and GlyOH-aq (3.214 mol cm^{-2} s^{-1}). The H_2 crossover rates at 100% RH exhibited the same trend. These results can be explained using the SAXS results in Fig. 3; the well-dispersed Nafion chains with small ionic clusters and narrow proton conducting channels can make the crossover of H_2 more difficult.

To make the effect of the solvent on the performance of the membrane more clear, the activation energies were calculated, and the relationship between the activation energies and the solubility parameters is presented in Fig. 7. After the RH declined from 100% to 30%, the activation energies for proton transport in membranes cast from 2-PrOH-aq, 1-PrOH-aq, EtOH-aq, MeOH-aq, NMP-aq, and GlyOH-aq increased significantly from approximately 9.5–17.9, 19.7, 20.7, 22.5, 20.3, and 24.1 kJ mol^{-1}, respectively. It is evident that the solubility parameters of the solvents had great effects on the activation energies, especially under low RH conditions, i.e., the activation energy for proton transportation in a proton exchange membrane becomes higher if the solubility parameter of the solvent is much farther away from the solubility parameter of Nafion.

3.3. *Effect of the solvent on the crystallinity and mechanical properties of the Nafion membranes*

The crystalline structures of the Nafion membranes that were made from different solutions were investigated with XRD. The diffraction peak between 15° and 21° can be resolved into two peaks (Fig. 8): a crystalline peak at approximately $2\theta = 17.5°$ and an amorphous peak [42]. The calculated results indicated that the crystallinity of the main chains of the polymer electrolyte increased if the solvent had a good intermiscibility with Nafion. The crystallinity of the membrane cast from GlyOH-aq was 10.58%. Using different solvents, the crystallinity values of the Nafion membranes increased to 16.7, 12.58, 11.68, 11.29, and 10.83% for membranes cast from 2-PrOH-aq, 1-PrOH-aq, EtOH-aq, NMP-aq and MeOH-aq, respectively. The increase in the crystallinity can be attributed to the well-dispersed PTFE like backbone and side chains in the solvent [30]. An improvement in the crystallinity further enhances the mechanical strengths of the membranes. Fig. 9a presents the stress–strain response of different Nafion membranes made from different solutions. The shape of the stress–strain curves can be approximately divided into two linear segments: the front segment reveals the yield strain, and the tail segment reveals the stress-to-failure. In general, the breaking strength of the membrane cast from 2-PrOH-aq reached 55 MPa, which was a much higher value than the 30 MPa breaking strength of the membrane cast from GlyOH-aq. However, the strain-to-failure values of these two membranes were almost the same (135%). The breaking strengths of the membranes made from 1-PrOH-aq, EtOH-aq, NMP-aq and MeOH-aq were 45 MPa, 40 MPa, 38 MPa, and 36 MPa, respectively. The strain-to-failure values were also different, as shown in Fig. 8a. The increase in the tensile strength may result from the stronger molecular bonding between the polymer chains. Thus, it indicates that the chain dispersion of Nafion could influence the microstructure of the corresponding membrane formed, and a solvent with a good intermiscibility allows the membrane to have a high resistance to stress.

The most important aspect of the physical durability for a proton exchange membrane is its humidity-induced stress under dynamic humidity levels. A recent study demonstrated that the safe fatigue strength of a pristine Nafion membrane is approximately 1.5 MPa.

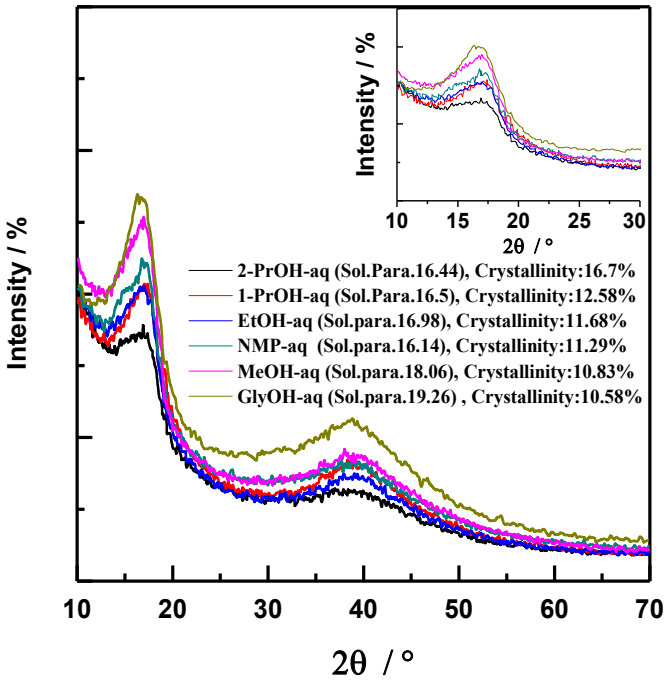

Fig. 8. XRD spectrum of membranes that prepared by different Nafion solutions.

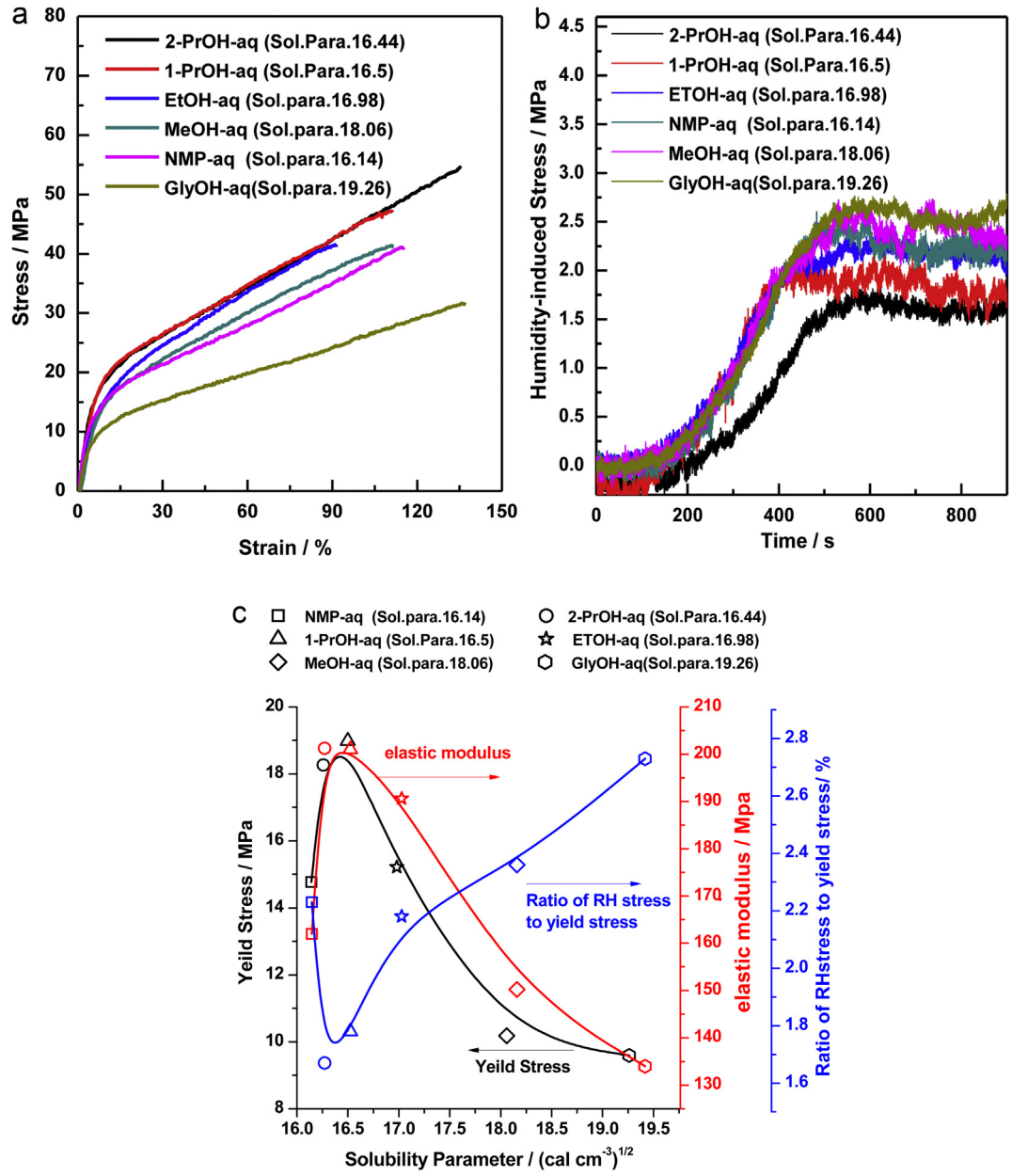

Fig. 9. Stress–strain responses (a), humidity-induced stress of the proton exchange membrane (b), and the physical stability of membrane that casted by different Nafion solutions (c).

When the fatigue strength of Nafion reaches 3.0 MPa, the dimension of the membrane changes significantly, and the microstructure easily breaks down after long-term operation [23]. Fig. 9b shows the humidity-generated stress of various membranes from a saturated state to a 25% RH at 25 °C. At the beginning of the test (0 s), the PEMs were water saturated by soaking them in DI water for 2 h at 25 °C, after which the liquid water on the membrane surface was removed. As shown in Fig. 9b, the humidity-induced stress values of the Nafion membranes that were prepared from different solutions including 2-PrOH-aq, 1-PrOH-aq, EtOH-aq, NMP-aq, MeOH-aq and GlyOH-aq were 1.5, 1.75, 2.0, 2.1, 2.25 and 2.5 MPa, respectively. These results suggest that a solvent with a good intermiscibility could promote the formation of a more compact and more organized molecular structure, lowering the shrinkage stress value near to the value for safe stress. The relationship between the physical stabilities of the membranes and the intermiscibilities of the solvents is presented in Fig. 9c. Because the solubility parameters of 2-PrOH-aq (16.44 (cal $cm^{-3})^{1/2}$) and 1-PrOH-aq (16.5 (cal $cm^{-3})^{1/2}$) are close to that of Nafion (16.45 (cal $cm^{-3})^{1/2}$), the membranes cast from both 2-PrOH-aq and 1-PrOH-aq exhibited compact molecular structures, which led to a high elastic modulus (approximately 200 MPa). For the other samples, the elastic modulus values of the membranes cast from EtOH-aq, MeOH-aq, NMP-aq, and GlyOH-aq were 190 MPa, 150 MPa, 163 MPa and 135 MPa, respectively. Moreover, the yield stress, which is shown in Fig. 9c, also proves that the dispersive behavior of PFSA had a great effect on the performance of PFSA membrane.

4. Conclusions

The microstructure of the proton exchange membrane is one of the very important issues that affects the electrochemical properties of the membrane. In this paper, the structures of

perfluorosulfonic acid membranes were studied by investigating the effect of solvents with various dielectric constants (ε) and solubility parameters (δ) on the dispersive behavior of the perfluorosulfonic acid resin. It was revealed that as the solubility parameter gap between the solvent and Nafion became larger, the particle clusters and the structure of their construction were changed from a regular distribution to a random dispersion with an increased aggregate size. The Nafion membrane cast from the Nafion-2-propanol/water dispersion exhibited better construction with an ordered ion cluster arrangement, smaller ion cluster size (approximately 13 Å), and higher crystallinity (16.7%) than those membranes made from other Nafion dispersions. The Nafion-2-propanol/water membrane had a compact and stable structure with a H_2 crossover rate approximately 0.5 mA cm^{-2} and a humidity-induced stress of approximately 1.5 MPa. Moreover, if the solvent has a higher ε than that of PFSA, δ becomes the main factor for the structural construction of the perfluorosulfonic acid membrane. Solvents with higher ε values can contribute to the formation of PFSA ionic aggregation much more than those with lower ε values.

Proton transport mechanisms are also discussed under different RHs along with the activation energy of proton transport. The vehicle mechanism is the main way that protons are transferred in the proton exchange membrane, whereas the effect of Grotthuss mechanism on the protonic transportation shows up gradually with the increase in RH. The PFSA solution with a solvent that had a good inter-miscibility had a strong positive effect on the physical stability of the corresponding proton exchange membrane that was formed.

Acknowledgments

This work is financially supported by the National Nature Science Foundation of China (51272200), Program for New Century Excellent Talents in University (NCET-12-0911) and the Fundamental Research Funds for the Central Universities (WUT: 2013-IV-037, 2013-II-011).

References

[1] M.S. Whittingham, R.F. Savinell, T. Zawodzinski, Chem. Rev. 104 (2004) 4243.
[2] K.A. Mauritz, R.B. Moore, Chem. Rev. 104 (2004) 4535–4585.
[3] H. Tang, Z. Wan, M. Pan, S.P. Jiang, Electrochem. Commun. 9 (2007) 2003–2008.
[4] C.M. Hansen, Prog. Org. Coat. 51 (2004) 77–84.
[5] E. Stefanis, C. Panayiotou, Int. J. Pharm. 426 (2012) 29.
[6] M. Laporta, M. Pegoraro, L. Zanderighi, Macromol. Mater. Eng. 282 (2000) 22–29.
[7] R.S. Yeo, Polymer 21 (1980) 432–435.
[8] H.L. Lin, T.L. Yu, C.H. Huang, T.L. Lin, J. Polym. Sci. Part B Polym. Phys. 43 (2005) 3044–3057.
[9] P. Aldebert, G. Gebel, B. Loppinet, N. Nakamura, Polymer 36 (1995) 431–434.
[10] H. Zhang, J. Pan, X. He, M. Pan, J. Appl. Polym. Sci. 107 (2008) 3306–3309.
[11] B. Loppinet, G. Gebel, Langmuir 14 (1998) 1977–1983.
[12] H.G. Haubold, T. Vad, H. Jungbluth, P. Hiller, Electrochim. Acta 46 (2001) 1559–1563.
[13] B. Loppinet, G. Gebel, C.E. Williams, J. Phys. Chem. B 101 (1997) 1884–1892.
[14] S.K. Young, S.F. Trevino, N.C.B. Tan, J. Polym. Sci. B Polym. Phys. 40 (2002) 387–400.
[15] L. Rubatat, G. Gebel, O. Diat, Macromolecules 37 (2004) 7772–7783.
[16] G. Gebel, R.B. Moore, Macromolecules 33 (2000) 4850–4855.
[17] S.-J. Lee, T.L. Yu, H.-L. Lin, W.-H. Liu, C.-L. Lai, Polymer 45 (2004) 2853–2862.
[18] C.-H. Ma, T.L. Yu, H.-L. Lin, Y.-T. Huang, Y.-L. Chen, U.S. Jeng, Y.-H. Lai, Y.-S. Sun, Polymer 50 (2009) 1764–1777.
[19] G.A. Giffin, G.M. Haugen, S.J. Hamrock, V. Di Noto, J. Am. Chem. Soc. 135 (2013) 822–834.
[20] Trung Truc Ngo, T. Leon Yu, Hsiu-Li Lin, J. Power Sources 225 (1 March 2013) 293–303.
[21] Y. Luan, Y. Zhang, L. Li, H. Zhang, Q. Zhang, Z. Huang, Y. Liu, J. Appl. Polym. Sci. 107 (2008) 2892.
[22] Z. Siroma, N. Fujiwara, T. Ioroi, S. Yamazaki, K. Yasuda, Y. Miyazaki, J. Power Sources 126 (2004) 41.
[23] R.F. Silva, M. De Francesco, A. Pozio, Electrochim. Acta 49 (2004) 3211.
[24] Klaus Schmidt-Rohr, Qiang Chen, Nat. Mater. 7 (2008) 75–83.
[25] M. Fujimura, T. Hashimoto, H. Kawai, Macromolecules 14 (1981) 1309–1315.
[26] P. Van der Heijden, L. Rubatat, O. Diat, Macromolecules 37 (2004) 5327–5336.
[27] H. Tang, S. Wang, M. Pan, S.P. Jiang, Y. Ruan, Electrochim. Acta 52 (2007) 3714–3718.
[28] G. Gebel, Polymer 41 (2000) 5829–5838.
[29] M.L. Einsla, Y.S. Kim, M. Hawley, H.-S. Lee, J.E. McGrath, B. Liu, M.D. Guiver, B.S. Pivovar, Chem. Mater. 20 (2008) 5636–5642.
[30] K.A. Page, K.M. Cable, R.B. Moore, Macromolecules 38 (2005) 6472–6484.
[31] H. Tang, P. Shen, S.P. Jiang, W. Fang, P. Mu, J. Power Sources 170 (2007) 85–92.
[32] T.D. Gierke, G.E. Munn, F.C. Wilson, J. Polym. Sci. Polym. Phys. Ed. 19 (1981) 1687–1704.
[33] C. Yang, P. Costamagna, S. Srinivasan, J. Benziger, A. Bocarsly, J. Power Sources 103 (2001) 1–9.
[34] C. Welch, A. Labouriau, R. Hjelm, B. Orler, C. Johnston, Y.S. Kim, ACS Macro Lett. 1 (2012) 1403–1407.
[35] G. Janssen, M. Overvelde, J. Power Sources 101 (2001) 117–125.
[36] K. Kreuer, J. Membr. Sci. 185 (2001) 29–39.
[37] A. Arico, V. Baglio, V. Antonucci, I. Nicotera, C. Oliviero, L. Coppola, P. Antonucci, J. Membr. Sci. 270 (2006) 221–227.
[38] D.X. Luu, E.-B. Cho, O.H. Han, D. Kim, J. Phys. Chem. B 113 (2009) 10072–10076.
[39] G.P. Robertson, S.D. Mikhailenko, K. Wang, P. Xing, M.D. Guiver, S. Kaliaguine, J. Membr. Sci. 219 (2003) 113–121.
[40] S.J. Paddison, R. Paul, T.A. Zawodzinski, J. Electrochem. Soc. 147 (2000) 617–626.
[41] N. Agmon, Chem. Phys. Lett. 244 (1995) 456–462.
[42] K.D. Kreuer, A. Rabenau, W. Weppner, Angew. Chem. Int. Ed. Engl. 21 (1982) 208–209.
[43] J. Lin, P.-H. Wu, R. Wycisk, P.N. Pintauro, Z. Shi, Macromolecules 41 (2008) 4284–4289.
[44] A.-L. Rollet, O. Diat, G. Gebel, J. Phys. Chem. B 106 (2002) 3033–3036.
[45] K.D. Kreuer, et al., J. Power Sources 178 (2008) 499–509.
[46] K.D. Kreuer, W. Weppner, A. Rabenau, Solid State Ionics 3/4 (1981) 353–358.
[47] J. Li, X. Yang, H. Tang, M. Pan, J. Membr. Sci. 361 (2010) 38–42.
[48] G. Alberti, R. Narducci, M. Di Vona, S. Giancola, Fuel Cells 13 (2013) 42–47.
[49] C. Francia, V.S. Ijeri, S. Specchia, P. Spinelli, J. Power Sources 196 (2011) 1833–1839.
[50] G. Gebel, P. Aldebert, M. Pineri, Macromolecules 20 (1987) 1425–1428.
[51] S. Kundu, M.W. Fowler, L.C. Simon, R. Abouatallah, N. Beydokhti, J. Power Sources 195 (2010) 7323–7331.
[52] S.S. Kocha, J. Deliang Yang, J.S. Yi, AIChE J. 52 (2006) 1916–1925.
[53] X. Cheng, J. Zhang, Y. Tang, C. Song, J. Shen, D. Song, J. Zhang, J. Power Sources 167 (2007) 25–31.